The Structural Unit of the Secretory $Na^+-K^+-2Cl^-$ Cotransporter (NKCC1) Is a Homodimer

Marilyn L. Moore-Hoon and R. James Turner*

Membrane Biology Section, Gene Therapy and Therapeutics Branch, National Institute of Dental and Craniofacial Research, National Institutes of Health, Bethesda, Maryland 20892

Received October 4, 1999; Revised Manuscript Received December 16, 1999

ABSTRACT: The oligomeric state of the secretory $Na^+-K^+-2Cl^-$ cotransporter (NKCC1) in rat parotid plasma membranes was studied using the reversible chemical cross-linker DTSSP [3,3′-dithiobis-(sulfosuccinimidyl propionate)]. The monomeric apparent molecular mass of NKCC1 is ∼170 kDa. However, we show here that this protein migrates as a ∼355 kDa complex on SDS−PAGE gels after membrane treatment with DTSSP, indicating that NKCC1 exists as an oligomer in the plasma membrane. The stability of this oligomer is such that it is not disrupted by solubilization of the membrane by low concentrations of the nonionic detergent Triton X-100 (0.3%) or the mild ionic detergent deoxycholate (20 mM); however, higher concentrations of Triton X-100 or treatment with the denaturing detergent SDS do result in destabilization of the NKCC1 complex. In additional experiments, we immunoprecipitated the 355 kDa cross-linked complex from biotinylated membranes, then cleaved the cross-linking bonds and analyzed the resulting components of the NKCC1 oligomer by avidin blotting, silver staining, and 2D electrophoresis. In these studies, we were unable to detect the presence of any proteins other than NKCC1 itself in the 355 kDa oligomer, suggesting that this complex is an NKCC1 dimer. Strong evidence for this conclusion was provided by a quantitative analysis of the molecular sizes of oligomers formed by full-length NKCC1 and an N-terminally truncated version of NKCC1 expressed in HEK293 cells. Taken together, our data provide convincing evidence that the dominant structural unit of NKCC1 in the plasma membrane is a homodimer.

It has recently been shown that a group of cation−chloride cotransporters make up a new gene family of membrane transport proteins (*1*−*3*). To date, seven members of this family have been identified in vertebrates: two $Na^+-K^+-2Cl^-$ cotransporter isoforms (NKCC1 and NKCC2),[1] one Na^+-Cl^- cotransporter (NCC), and four K^+-Cl^- cotransporter isoforms (KCC1, KCC2, KCC3, and KCC4). All of these proteins are electroneutral salt transporters, and their established physiological roles include (*1, 2, 4*−*6*) involvement in transepithelial salt and water movements, cell volume regulation, control of intracellular [Cl^-], and the transport of NH_4^+ (and thereby acid/base equivalents). Members of this gene family have also been identified in worms, plants, insects, yeast, and a cyanobacterium (*7*−*9*), but the functions of these homologous proteins have not yet been established. Hydropathy analyses predict that all of these transporters have a similar membrane topology consisting of large hydrophilic N- and C-termini on either side of a central hydrophobic transmembrane region. This transmembrane region is predicted to consist of 10−12 membrane-spanning domains (*10*) which are presumed to be α-helices.

Thus far, most of the molecular-level experimental information concerning the structure and function of cation−chloride transporters has come from studies of NKCC1, the "secretory" isoform of the $Na^+-K^+-2Cl^-$ cotransporters. This transporter is relatively widely expressed in both epithelial and nonepithelial tissues (*11*−*13*). It has been of considerable interest because of its roles in cell volume regulation and as the Cl^- entry step in many Cl^- secretory epithelia (*1, 2, 6*). Evidence for the cytosolic location of the N- and C-termini of NKCC1 has come from antibody accessibility studies (*10*) as well as experiments that localize sites of regulatory phosphorylation to these domains (*1*, *14*−*16*). Sites of N-linked glycosylation have been identified in the loop between predicted membrane-spanning regions 7 and 8, indicating that the loop is extracellular (*17*). Also, in an elegant series of experiments, Isenring, Forbush, and collaborators have used chimeras and point mutations to explore the role of various regions of NKCC1 in ion translocation and inhibitor binding (*18*−*20*). Briefly stated, these studies show that predicted membrane-spanning regions 2, 4, and 7 contain essential residues associated with the ion transport affinities of NKCC1 and that residues in these as well as other more C-terminal membrane-spanning regions affect the binding affinity of the $Na^+-K^+-2Cl^-$ cotrans-

* Address correspondence to this author at Building 10, Room 1A06, 10 Center Dr., MSC 1190, National Institutes of Health, Bethesda, MD 20892-1190. Tel: (301) 402-1060, FAX: (301) 402-1228, e-mail: rjturner@nih.gov.

[1] Abbreviations: NKCC, $Na^+-K^+-2Cl^-$ cotransporter; NCC, Na^+-Cl^- cotransporter; KCC, K^+-Cl^- cotransporter; DTSSP, 3,3′-dithiobis-(sulfosuccinimidyl propionate); PBS, phosphate-buffered saline; Sulfo-NHS-Biotin, sulfosuccinimidobiotin; AEBSF, 4-(2-aminoethyl)benzenesulfonyl fluoride hydrochloride; PMSF, phenylmethylsulfonyl fluoride; TPCK, L-tosylamido-2-phenylethyl chloromethyl ketone; EDTA, ethylenediaminetetraacetic acid; EGTA, ethylene glycol bis-(β-aminoethyl ether)-*N*,*N*,*N*′,*N*′-tetraacetic acid; HEPES, *N*-(2-hydroxyethyl)piperazine-*N*′-2-ethanesulfonic acid.

10.1021/bi992301v CCC: $19.00
Published on Web 03/10/2000

porter inhibitor bumetanide. The cytosolic N- and C-termini, on the other hand, appear to have little effect on these properties of NKCC1 (*20*) and may instead be mainly involved in the regulation of transport activity.

To begin to integrate this structural and functional information into a working model of the operation of NKCC1, it is essential to know the composition of the NKCC1 structural unit in the membrane. In this regard, it has been shown that a number of membrane transport proteins are oligomeric. Among the better studied examples are the Na^+/K^+ and H^+/K^+ ATPases (*21*), the Na^+/H^+ exchanger (*22*), the erythrocyte Cl^-/HCO_3^- exchanger (*23*), the epithelial sodium channel (*24*), and the aquaporins (*25*). Using chemical cross-linking studies, we demonstrate here that NKCC1 also exists as an oligomer in the plasma membrane and that this complex remains intact after gentle detergent solubilization. A number of additional observations, including studies of the oligomerization of an N-terminally truncated NKCC1, indicate that NKCC1 forms a homodimer.

MATERIALS AND METHODS

Materials. Phosphate-buffered saline (PBS: 1.7 mM KH_2PO_4, 5 mM Na_2HPO_4, 150 mM NaCl, pH 7.4 with NaOH) was obtained from Digene Diagnostics (Silver Spring, MD). DTSSP [3,3′-dithiobis(sulfosuccinimidyl propionate)], Sulfo-NHS-Biotin (sulfosuccinimidobiotin), and Protein G Sepharose beads were from Pierce (Rockford, IL). Endoglycosidase-F/N-glycosidase F, pepstatin, and leupeptin were from Boehringer Mannheim (Indianapolis, IN). AEBSF [4-(2-aminoethyl)benzenesulfonyl fluoride hydrochloride] was from ICN (Aurora, OH). Ovalbumin, PMSF (phenylmethylsulfonyl fluoride), and TPCK (L-tosylamido-2-phenylethyl chloromethyl ketone) were from Sigma (St. Louis, MO), and bestatin was from Calbiochem (La Jolla, CA). All other chemicals were from standard commercial sources and were reagent grade or the highest purity available.

Protein was measured using the Bio-Rad Protein Assay Kit (Bio-Rad, Hercules, CA) using bovine IgG as the standard.

Membrane Preparations. A crude membrane fraction was prepared from rat parotid glands by differential centrifugation as previously described (*26*). Briefly stated, finely minced glands suspended in a medium consisting of 10 mM HEPES (pH 7.4 with Tris), 10% sucrose, 1 mM EDTA, and 0.1 mM PMSF were homogenized using a polytron (Brinkmann Instruments, Westbury, NY) and then centrifuged at 2500*g* for 5 min. The supernatant was saved, and the pellet was resuspended in the same medium and rehomogenized and respun. This was repeated for a total of 4 homogenization steps. The combined supernatants were then centrifuged at 22000*g* for 20 min, and the resulting pellet was resuspended at 10 mL/g starting parotid mince in PBS containing 1.5 μM pepstatin, 100 μM TPCK, 10 μM leupeptin, and 1 μM bestatin (PBSp). This material was centrifuged again at 43700*g* for 20 min, resuspended in 1 mL of PBSp/g of starting mince, and passed once through a 25 gauge needle and once through a 30 gauge needle before being snap-frozen in liquid nitrogen into 100 μL aliquots. These aliquots (typically containing >10 mg of membrane protein/mL) were stored over liquid nitrogen until use.

Crude membranes from HEK-293 cells were prepared as follows. The cells growing in a 10 cm culture dish were washed twice in ice-cold PBS containing 1 mM EGTA then scraped into 1 mL of the same medium. This material was centrifuged at 1000*g* for 5 min; then the supernate was removed and the pellet frozen and stored above liquid nitrogen. On the day of the cross-linking experiment, the pellet was thawed, resuspended in 1 mL of TEEA (20 mM Tris-HCl, pH 8.0, containing 1 mM EDTA, 3 mM EGTA, and 300 μM AEBSF), and homogenized by passing 4 times through a 25 gauge needle. This material was centrifuged at 1000*g* for 5 min and the supernate saved. The pellet was resuspended in TEEA and rehomogenized and centrifuged as before. The combined supernates from these two homogenization steps were centrifuged at 100000*g* for 30 min, and the resulting membrane pellet was resuspended in 300 μL of PBS.

Cross-Linking and Biotinylation of Membrane Proteins. Chemical cross-linking and biotinylation studies were carried out in conjunction with immunoprecipitation and Western blotting (see below) in order to determine whether NKCC1 was closely associated with (and thus could be cross-linked to) other membrane proteins. Rat parotid or HEK-293 cell crude membranes prepared as described above were diluted to a final protein concentration of 1 mg/mL in PBS and other additions as indicated and cross-linked on ice using the water-soluble, cleavable amino reagent DTSSP. An amino reagent was chosen for these studies because rat NKCC1 contains 70 lysine residues (*10*), 56 of which are found in the intracellular N- and C-termini of the molecule; thus, it was anticipated that there would be ample potentially available cross-linking sites. When utilized, detergents were added to the reaction mixture 30 min prior to DTSSP (see figure captions). The cross-linking reaction (typically carried out with 1 mM DTSSP for 35 min) was terminated by the addition of an equal volume of stop solution consisting of 100 mM glycine, 0.6% Triton X-100, and 0.5 mM PMSF in PBSp.

To simultaneously biotinylate and cross-link membrane proteins, rat parotid membranes (1 mg of protein/mL in PBS plus 0.3% Triton X-100) were first incubated for 5 min on ice in the presence of 0.2 mg/mL Sulfo-NHS-Biotin after which 1 mM DTSSP was added and incubation was continued for an additional 2 h. The reaction was then stopped by the addition of 1 volume of the same stop solution used for the cross-linking reaction. In all cross-linking and biotinylation plus cross-linking experiments, the membranes were left on ice for 10 min after the addition of the stop solution before additional experimental steps were carried out.

Immunoprecipitation of the Biotinylated Cross-Linked Rat Parotid NKCC1. Immunoprecipitation was carried out using the antibody α-wCT which was raised in rabbits against a 6×His fusion protein corresponding to amino acids 750−1203 of the rat NKCC1 (*10*). α-wCT was preconjugated to protein G beads as follows. Protein G beads were first washed 4 times in PBSp containing 1% ovalbumin. Next 1 volume of serum was combined with 3 volumes of beads and 17 volumes of PBSp plus 1% ovalbumin and incubated at 4 °C for 1 h with constant mixing. The beads were then washed 4 times with PBSp plus 1% ovalbumin, 0.3% Triton X-100, and 0.25 mM PMSF and dispensed into suitable aliquots. Biotinylated cross-linked membranes (see above) to be subjected to immunoprecipitation were diluted 1:1 with

PBSp containing 50 mM glycine, 0.3% Triton X-100, 0.25 mM PMSF, and 2% ovalbumin and clarified by centrifugation at 13000*g* for 5 min; then 450 μL of the resulting supernatant was added to 13.3 μL of preconjugated beads. Following 2 h of incubation at 4 °C, the beads were collected by centrifugation and washed 3 times in PBSp containing 0.3% Triton X-100 and 1% ovalbumin and 4 times in PBS containing 0.3% Triton X-100, changing the tube on the last wash. The final pellet of beads was either extracted with sample buffer for SDS−PAGE or subjected to further treatment as described below before SDS−PAGE analysis.

Deglycosylation of Immunoprecipitated Material and Cleavage of DTSSP. Deglycosylation of immunoprecipitated NKCC1 on protein G beads was carried out using endoglycosidase-F/N-glycosidase F by adding 20 μL of the enzyme (as supplied by the manufacturer) diluted 5-fold with 20 mM potassium phosphate buffer (pH 7.5) to the above final pellet of protein G beads (0.2 unit of enzyme/13.3 μL of beads) and incubating for 60 min at 37 °C. Nondeglycosylated controls were treated identically but with 20 mM potassium phosphate buffer replacing the glycosidase solution. Cleavage of DTSSP was carried out by adding 100 mM DTT and incubating an additional 30 min at 37 °C.

SDS−PAGE, Western Blotting, and Silver Staining. SDS−PAGE was carried out using 4−12% Tris−glycine gels from Novex (San Diego, CA). No sulfhydryl reducing agents were added to the SDS−PAGE loading buffer. Gels to be Western blotted were transferred to nitrocellulose (Schleicher & Schuell, Keene, NH) in a Novex XCell II Mini-Cell using 192 mM glycine, 25 mM Tris (pH 8.8) as the transfer buffer. Immunoblotting was carried out in 25 mM Tris-HCl, pH 7.5, containing 140 mM NaCl, 4% skim milk powder (Giant Foods, Rockville, MD), and 0.04% Tween 20 (Tween 20 was omitted during incubation with the primary antibody). The primary and secondary antibodies were α-wCT, used at a dilution of 1:15 000, and horseradish peroxidase-conjugated goat anti-rabbit IgG (Pierce), used at a dilution of 1:30 000, respectively. Detection was carried out using the ECL kit from Amersham (Arlington Heights, IL) according to the manufacturer's directions. The positions of the BioRad High Range Prestained SDS−PAGE standards are indicated on the blots.

Detection of biotin-labeled proteins by Western blotting was carried out as described above except that horseradish peroxidase-conjugated Immunopure Avidin (Pierce), used at a dilution of 1:1000, replaced the primary antibody and no secondary antibody was used.

Gels were silver stained using the Amersham (Arlington Heights, IL) Quicksilver Detection Kit following the manufacturer's instructions. The positions of the BioRad High Range Silver Stain SDS−PAGE standards are indicated on the silver-stained gels.

2-D Gel Analysis. Two-dimensional electrophoresis was performed according to the method of O'Farrell (*27*) by Kendrick Labs, Inc. (Madison, WI). The resulting gel was transferred onto nitrocellulose using the same methanol-free transfer buffer described above. Calibration of the gel using appropriate isoelectric focusing and molecular weight standards was carried out by Kendrick Labs.

Expression of NKCC1 and N-Terminally Truncated NKCC1 in HEK293 Cells. The mammalian expression vector pBK-CMV^{lac-} was used for expression studies in HEK293 cells;

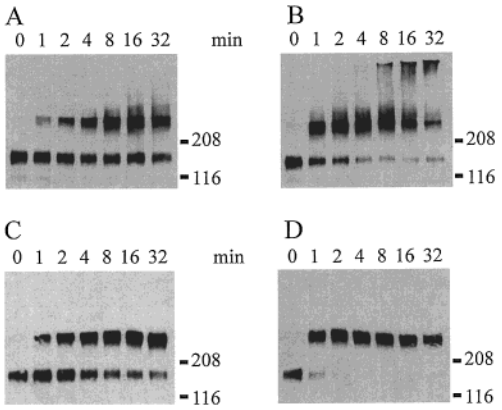

FIGURE 1: Time course of cross-linking of the rat parotid NKCC1 protein by DTSSP. Parotid membranes, pretreated for 30 min in the absence (panels A and B) or presence (panels C and D) of 0.3% Triton X-100, were cross-linked (see Materials and Methods) with 0.1 mM DTSSP (panels A and C) or 1.0 mM DTSSP (panels B and D) for the times indicated. The resulting samples were then analyzed by nonreducing SDS−PAGE and Western blotting using the anti-rat NKCC1 antibody α-wCT as described under Materials and Methods. In all cases, the bottom portions of the sample loading wells of the gels are included on the blot.

pBK-CMV^{lac-} was prepared from the vector pBK-CMV (Stratagene, La Jolla, CA) by removing the prokaryotic expression cassette as suggested by the manufacturer. A full-length NKCC1 construct was obtained by ligating the 5′-end of the mouse NKCC1 clone (*12*) kindly provided by Dr. E. Delpire, excised with *Eco*RI and *Fsp*I (610 bp of coding sequence), and the 3′-end of the rat NKCC1 (*10*), excised with *Fsp*I and *Xho*I (3005 bp of coding sequence), into pBK-CMV^{lac-} previously digested with *Eco*RI and *Xho*I. Note that at the time of making this construct the full 5′-end of the rat NKCC1 was not available; consequently, we utilized this mouse/rat chimera for in vitro transfection studies. The mouse and rat NKCC1's are 95% identical at the amino acid level (*10*). An N-terminally truncated NKCC1 construct was obtained by ligating the rat NKCC1 excised with *Fsp*I and *Xho*I into pBK-CMV^{lac-} previously digested with *Hin*dIII and treated with the Klenow fragment of DNA polymerase I to form blunt ends, then digested with *Xho*I. This results in an open reading frame which begins at the second methionine (Met-209) of the rat NKCC1. This N-terminally truncated construct codes for the last 995 amino acids of NKCC1 while the full-length NKCC1 codes for 1205 amino acids.

HEK-293 cells growing in IMEM (Biofluids, Rockville, MD), supplemented with 10% heat-inactivated fetal bovine serum, 2 mM glutamine, and 100 μM each of penicillin and streptomycin, were transfected with the above constructs using the MBS Mammalian Transfection Kit (Stratagene) following the manufacturer's instructions. Stable transfectants were selected by growth in the presence of 0.2 mg/mL G418 (Gibco BRL, Rockville, MD) and cloned by limiting dilution.

RESULTS AND DISCUSSION

Cross-Linking with DTSSP Demonstrates That NKCC1 Exists as a Dimer in the Plasma Membrane. Panels A and B of Figure 1 show the results of experiments where rat parotid membranes were incubated for various times (from 0 to 32 min) with 0.1 or 1 mM, respectively, of the cross-linker DTSSP. Following the cross-linking reaction, the

mobility of the parotid NKCC1 on SDS−polyacrylamide gels was determined by Western blotting as described under Materials and Methods. Before reaction with DTSSP, we observe a single band at ~170 kDa, the previously documented monomeric molecular mass of this protein (*28*). Incubation with 0.1 mM DTSSP (panel A) results in the appearance of a higher molecular mass immunoreactive band whose intensity gradually increases with time. As discussed in detail later in the paper, we have estimated the apparent molecular mass of this latter band to be ~355 kDa by extrapolation of the mobility of known molecular mass standards. Accordingly, for simplicity, we refer to this higher molecular mass immunoreactive species as the '355 kDa complex' in what follows.

In the presence of 1 mM DTSSP (panel B), the rate of appearance of the 355 kDa complex is increased over that seen in panel A, and after 4 min of incubation, virtually all of the immunoreactive signal has migrated from 170 to 355 kDa. Thereafter, there is a gradual appearance of very high molecular mass immunoreactive species that remain at or near the top of the gel while the signal at 355 kDa is simultaneously lost. When these same treatments are carried out in the presence of 0.3% Triton X-100 (panels C and D), very similar results are found except that the appearance of the 355 kDa band is somewhat less diffuse and it is not lost to higher molecular mass species in the presence of 1 mM DTSSP (cf. panels B and D).

The experiments illustrated in Figure 1 indicate that NKCC1 is closely associated with another protein, or proteins, in the parotid membrane to which it is readily cross-linked to form the 355 kDa complex. The association between these proteins is sufficiently strong that it is not disrupted by 0.3% Triton X-100 (panels C and D), a concentration of detergent that results in the complete solubilization of the cotransporter under our experimental conditions (*28, 29*). The very high molecular mass immunoreactive species seen after longer incubations of intact membranes with 1 mM DTSSP (panel B) are presumably due to the nonspecific cross-linking of many membrane proteins into large aggregates. Consistent with this interpretation, when the membrane is dissociated by solubilization (panels C and D), these aggregates are no longer seen. The results shown in Figure 1 also suggest that the 355 kDa cotransporter complex is a dimer since there is no indication of the presence of any intermediate bands between the 170 kDa monomer and the 355 kDa band under any of the experimental conditions illustrated (if the 355 kDa complex were a multimer, one would expect to see intermediate bands representing the cotransporter plus various subsets of the other proteins making up the multimer). It should also be noted that this dimer does not arise as the result of disulfide bond formation since the SDS−PAGE gels employed in Figure 1 were run in the absence of sulfhydryl reducing agents (see Materials and Methods) and the un-cross-linked cotransporter runs as a monomer under these conditions.

In the experiments shown in the three left-hand lanes of Figure 2A, we examine the effects of several other detergents on the stability of the 355 kDa complex. In each case, the detergents have been used at concentrations that are commonly employed to solubilize membrane proteins and that are well above their critical micelle concentrations. When rat parotid membranes were pretreated with the zwitterionic

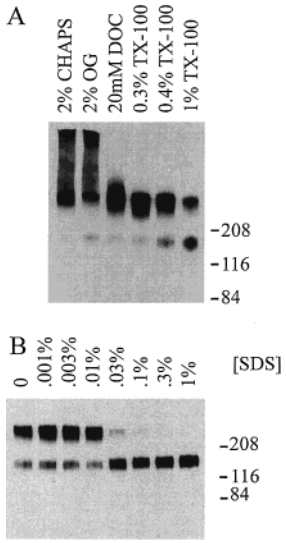

FIGURE 2: Effect of detergents on cross-linking of rat parotid NKCC1 by DTSSP. In panel A, parotid membranes were treated for 30 min on ice with the detergents CHAPS, octyl glucoside (OG), sodium deoxycholate (DOC), and Triton X-100 (TX-100) at the concentrations indicated, and then cross-linked with 1 mM DTSSP for 35 min as described under Materials and Methods. In panel B, parotid membranes were solubilized for 30 min on ice with 0.3% Triton X-100 and then treated for an additional 30 min with the concentrations of SDS indicated, before cross-linking. Following termination of the cross-linking reactions, the resulting samples were analyzed by nonreducing SDS−PAGE and Western blotting using the anti-rat NKCC1 antibody α-wCT as described under Materials and Methods.

detergent CHAPS or the nonionic detergent octyl glucoside (OG) and then cross-linked with DTSSP, a band of NKCC1 immunoreactivity was found at 355 kDa, but a smear of immunoreactivity was also seen above the 355 kDa band extending to very high molecular masses. These results suggest, somewhat surprisingly, that both of these detergents result in the aggregation of NKCC1 with itself or with other membrane proteins under the experimental conditions employed here. On the other hand, an intact 355 kDa complex was detected following solubilization of the membrane with the mild ionic detergent deoxycholate (DOC) at 20 mM concentration. We also illustrate in the three right-hand lanes of Figure 2A that some dissociation of the 355 kDa band is observed at concentrations of Triton X-100 $\geq$0.4%, indicating that the interactions that stabilize this complex can be disrupted by sufficiently high Triton concentrations.

Since the un-cross-linked cotransporter runs as a monomer on SDS−PAGE gels (Figure 1), we know that the 355 kDa complex can be dissociated by SDS. This effect is explored in more detail in Figure 2B where we examine the effect of increasing concentrations of SDS on the stability of the Triton X-100 solubilized complex. In these experiments, an abrupt change between the complexed and uncomplexed cotransporter was consistently seen as the SDS concentration was increased from 0.01% to 0.03%.

Evidence That NKCC1 Is the Only Component of the 355 kDa Complex. We next set out to determine whether the 355 kDa complex was a homodimer or a heterodimer. Our first experiments were designed to search for evidence of proteins other than NKCC1 in the cross-linked complex. We did this by biotinylating and cross-linking solubilized rat parotid membranes, immunoprecipitating the 355 kDa complex with

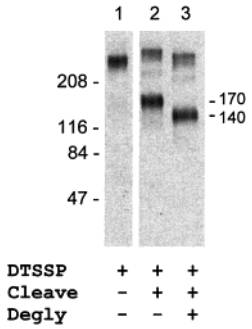

FIGURE 3: Components of the cross-linked NKCC1 355 kDa complex. Rat parotid membranes solubilized in 0.3% Triton X-100 were biotinylated using Sulfo-NHS-Biotin and cross-linked with DTSSP; then the 355 kDa complex was immunoprecipitated using the antibody α-wCT. This immunoprecipitated material was either run directly on SDS−PAGE (lane 1), treated with 100 mM DTT to cleave the cross-linking bonds and then run on SDS−PAGE (lane 2), or deglycosylated and treated with DTT to cleave DTSSP bonds before running on SDS−PAGE (lane 3). The resulting gel was analyzed by Western blotting using horseradish peroxidase-conjugated avidin. The three lanes shown are from the same blot. All procedures are described under Materials and Methods.

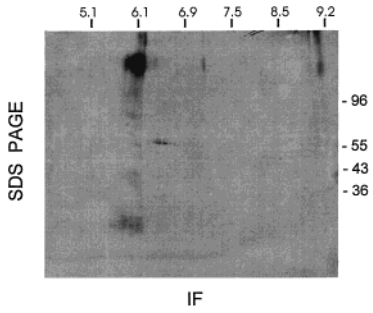

FIGURE 4: Two-dimensional gel analysis of the components of the deglycosylated NKCC1 355 kDa complex. The immunoprecipitated, deglycosylated, cleaved 355 kDa complex prepared as described for lane 3 of Figure 3 was subjected to 2-D electrophoresis and avidin blotting as described under Materials and Methods.

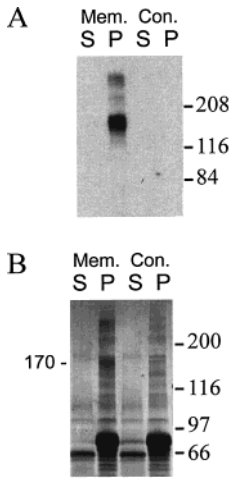

FIGURE 5: Release of components of the 355 kDa complex by 0.1% SDS. Rat parotid membranes solubilized in 0.3% Triton X-100 were biotinylated using Sulfo-NHS-Biotin and cross-linked with DTSSP; then the 355 kDa complex was immunoprecipitated using the antibody α-wCT. The resulting protein G bead pellet was suspended in 20 μL of PBS containing 0.3% Triton X-100 and 100 mM DTT and incubated for 30 min at 37 °C to cleave cross-linking bonds. SDS was then added to a final concentration of 0.1%, and, after a further 30 min incubation, the protein G beads were spun down, and the supernatant was removed. SDS sample buffer was added to both supernatant (S) and pellet (P) to give a final volume of 40 μL in each case, and equal volumes of both samples were run on two SDS−PAGE gels, one to be used for avidin Western blotting (panel A) and the other for silver staining (panel B). In addition to these samples containing cross-linked parotid membranes (Mem.), control samples (Con.) without membranes but otherwise identically treated were processed in parallel.

an anti-rat NKCC1 antibody, and then cleaving the cross-linking bonds and looking for evidence of multiple biotinylated cleavage products (see Materials and Methods for details). The results of such an experiment are shown in Figure 3. Lane 1 shows the cross-linked biotinylated cotransporter, and lane 2 shows its cleavage products. A biotinylated band at ∼355 kDa is seen in lane 1 as expected. In lane 2, a band representing a biotinylated protein at ∼170 kDa whose diffuse appearance is similar to that of NKCC1 is clearly seen (cf. Figures 1 and 2); however, there is no evidence for the presence of any other proteins with molecular masses ≲170 kDa that could be components of the 355 kDa complex. In lane 3, we show the deglycosylated cleavage products of the 355 kDa complex. It has been previously demonstrated that NKCC1 is heavily glycosylated and a downward shift in apparent molecular mass of ∼30 kDa is expected upon deglycosylation (*29*, *30*). Consistent with the identification of the 170 kDa band in lane 2 with NKCC1, we see a biotinylated band at ∼140 kDa in lane 3 (the molecular mass of unglycosylated NKCC1 is predicted to be 130 kDa from its amino acid sequence), but again there is no evidence for the presence of any other proteins with molecular masses ≲170 kDa that could be components of the 355 kDa complex.

To further characterize the 140 kDa band seen in lane 3 of Figure 3, we analyzed this cleaved deglycosylated material by two-dimensional gel electrophoresis. The resulting avidin blot (Figure 4) shows a single spot at ∼140 kDa with p*I* ≈ 6.1 (the predicted p*I* of the rat NKCC1 is 6.5 but note that the material used to obtain Figure 4 had been previously reacted with Sulfo-NHS-Biotin, DTSSP, and DTT, any of which could have an effect on the p*I*). Thus, the results shown in Figures 3 and 4 provide strong evidence that the 355 kDa complex is a dimer made up of NKCC1 and a second protein with properties virtually identical to NKCC1, namely, the same apparent molecular mass, the same shift in apparent molecular mass following deglycosylation, and the same p*I*.

In another series of experiments (Figure 5), we immunoprecipitated the biotinylated cross-linked 355 kDa complex and cleaved the cross-linking bonds as before, then looked for proteins that were released from the immune complex by 0.1% SDS. This was done by spinning down the antibody-conjugated protein G beads following cleavage of cross-linking bonds and SDS treatment, and analyzing the resulting supernatant by SDS−PAGE, avidin Western blotting, and silver staining. Our rationale here was that, since the 355 kDa complex is completely disrupted by 0.1% SDS (Figure 2B), any non-NKCC1 proteins should be released by this treatment. However, in these experiments, we were unable to detect the presence of any such released proteins with either avidin blotting (Figure 5A, first lane on left) or silver staining (Figure 5B, compare first and third lanes from the left; see figure caption for details). This result is consistent with the hypothesis that the 355 kDa complex contains only NKCC1 proteins that therefore remain bound to the anti-

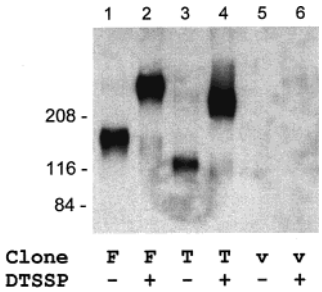

FIGURE 6: Effect of truncating NKCC1 on the apparent molecular mass of the cross-linked cotransporter. Membranes from HEK293 cells stably transfected with a full-length NKCC1 (F), an N-terminally truncated NKCC1 (T), and a vector control (pBK-CMV^{lac-} with no insert; v) were solubilized in 0.3% Triton X-100 and treated with (+) or without (−) DTSSP, as indicated, and then analyzed by SDS−PAGE and Western blotting using the anti-rat NKCC1 antibody α-wCT. All procedures are described under Materials and Methods.

NKCC1 antibody on the protein G beads. Taken together with the results of Figures 3 and 4, these observations strongly suggest that the 355 kDa complex is an NKCC1 homodimer.

Direct Evidence That the Structural Unit of NKCC1 Is a Homodimer. In Figure 6 we show the results of cross-linking experiments carried out on membranes from HEK293 cells stably transfected (see Materials and Methods) with a full-length NKCC1 (F), an N-terminally truncated NKCC1 (T), and a vector control (v). In each case, membranes were treated with (+) or without (−) DTSSP, as indicated, and analyzed by SDS−PAGE and Western blotting. We note first that NKCC1 clearly dimerizes in HEK293 cells (Figure 6, lane 2), suggesting that this phenomenon is a general characteristic of this protein rather than an effect specific to parotid acinar cells. Furthermore, the N-terminally truncated NKCC1 also dimerizes (Figure 6, lane 4), indicating that the N-terminal 210 amino acids of NKCC1 are not required for this interaction. A decrease in apparent molecular mass of both the truncated NKCC1 and the truncated cross-linked product is seen relative to the corresponding full-length constructs. No significant immunoreactive signal is seen in membranes from HEK293 cells transfected with the vector control (lanes 5 and 6).

The results from three independent experiments of the type shown in Figure 6 are quantitated in Figure 7. Here we have determined the relative mobilities (R_f) of the four immunoreactive species and the SDS−PAGE molecular mass standards run in each experiment by normalizing the mobilities of all proteins to that of the 116 kDa standard. Analyzed in this way, these experiments were found to be highly reproducible (SEM's on R_f values were typically $\lesssim$1%; see below). It has previously been shown (*31*) that a plot of the logarithm of the molecular weight vs the square root of R_f for proteins run on SDS−PAGE gradient gels is linear over a broad range of molecular weights (10^4−10^6). As illustrated in Figure 7, such a plot for the molecular mass standards run in our experiments (solid circles) is clearly linear. The solid line drawn through these points was obtained by least-squares regression analysis ($R = 0.9995$). This least-squares fit was used to calculate the apparent molecular masses (crosses) of the various immunoreactive species shown in Figure 6. The results are 167 ± 10 kDa for the NKCC1 monomer, 125 ± 7 kDa for the N-terminally truncated

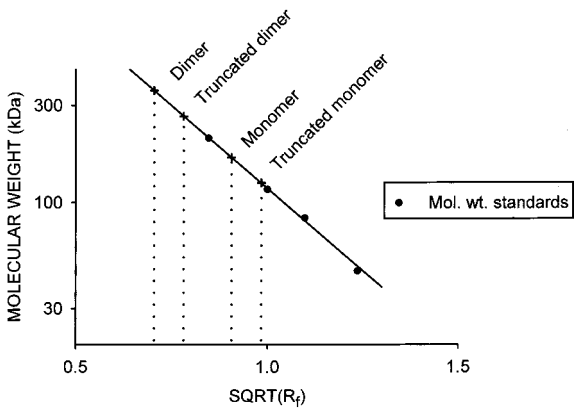

FIGURE 7: Determination of the apparent molecular masses of the monomeric and dimeric NKCC1 and truncated NKCC1. The relative mobilities (R_f) of the four immunoreactive species and the molecular mass standards run in three independent experiments of the type shown in Figure 6 were determined by normalizing the mobilities of all proteins to that of the 116 kDa standard. In the figure, the molecular mass (on a semilogarithmic scale) of each protein standard has been plotted vs the square root (SQRT) of its R_f (solid circles). The solid line drawn through these points was obtained by least-squares regression analysis. Also indicated (by crosses) are the points at which the relative mobilities of the various immunoreactive species lie on the regression line. The experimental variability (SEM) on all points (molecular mass standards and immunoreactive species) is smaller than the symbols shown in the figure.

NKCC1 monomer, 355 ± 18 kDa for the full-length dimer, and 266 ± 14 kDa for the dimer formed from the truncated NKCC1 (the relative mobilities of these species used for this calculation were 0.820 ± 0.010, 0.969 ± 0.012, 0.495 ± 0.003, and 0.610 ± 0.013, respectively). From these results, we can see that the apparent molecular masses of the two dimers are very close to twice the molecular masses of the corresponding monomers, consistent with the hypothesis of homodimers. More significantly, we find that the difference in molecular masses between the dimers formed from full-length and truncated NKCC1 (89 ± 23 kDa) is significantly larger than the difference in molecular masses between the corresponding monomers (42 ± 12 kDa). This latter observation argues strongly in favor of homodimers since the difference in molecular mass between heterodimers would have to be equal to that between the two monomers.

CONCLUDING REMARKS

We demonstrate here that the secretory $Na^+-K^+-2Cl^-$ cotransporter, NKCC1, whose monomeric molecular mass is 170 kDa, exists as a 355 kDa complex in the plasma membrane (Figures 1 and 7). The stability of this oligomer is such that it is not disrupted by solubilization of the membrane by low concentrations (~0.3%) of the nonionic detergent Triton X-100; however, higher concentrations of Triton X-100 or treatment with the denaturing detergent SDS do result in destabilization of the cotransporter complex (Figures 1 and 2). Our experiments also show that there is no evidence for the presence of multiple protein species in the 355 kDa complex (Figures 3−5), suggesting that it is an NKCC1 homodimer. Strong evidence for this conclusion is provided by the observation that when an N-terminally truncated version of the cotransporter is expressed in HEK293 cells the apparent molecular mass of the resulting cross-linked complex is consistent with that of a homodimer

and not a heterodimer (Figures 6 and 7). Recently it has been shown that the absorptive isoform of the $Na^+-K^+-2Cl^-$ cotransporter, NKCC2, whose monomeric molecular mass is ~160 kDa, is likewise present as a ~300 kDa oligomer in renal membranes (*32*). Although the composition of this oligomer has not been determined, this observation suggests that other members of the cation−chloride cotransporter gene family may also form homodimers.

Our experiments indicate that little or none of the NKCC1 protein in the rat parotid membrane, or in membranes from NKCC1-transfected HEK293 cells, exists in monomeric form. In addition, we see little or no evidence for trimers or higher order oligomers. Thus, a homodimer appears to be the dominant structural unit for NKCC1. Our studies do not address the related question of whether individual NKCC1 subunits within a dimer function cooperatively or independently of one another. However, all of the data to date indicate that functional $Na^+-K^+-2Cl^-$ cotransporting units operate independently. Thus, for example, not only is the stoichiometry of $Na^+-K^+-2Cl^-$ cotransport $1Na^+:1K^+:2Cl^-$, but also the dependence of flux on sodium concentration is hyperbolic (*13*, *33*, *34*), indicating that only one sodium ion is *involved* in the cotransport event. A similar hyperbolic dependence of flux on potassium concentration is also found (*13*, *33*, *34*). These observations are inconsistent with a cooperative association of two $Na^+-K^+-2Cl^-$ cotransporting units where the interaction of Na^+ (or K^+) with one transporting unit would affect the properties of the other. Bumetanide binding to $Na^+-K^+-2Cl^-$ cotransporters has also been shown to be a hyperbolic function of both sodium and potassium concentrations (*35*, *36*), indicating that only one Na^+ and one K^+ are involved in the bumetanide binding event. Thus, these functional data are consistent with the hypothesis that individual NKCC1 subunits within a dimer operate independently as $Na^+-K^+-2Cl^-$ cotransporters, or, alternatively, that a dimer is a single functional $Na^+-K^+-2Cl^-$ cotransporting unit that can bind one bumetanide molecule and carry out the cotransport of one sodium, one potassium, and two chloride ions. Additional experiments will be required to distinguish between these possibilities.

ACKNOWLEDGMENT

We thank Drs. Bruce Baum and Mark Knepper for helpful discussions and encouragement during the course of this work, and Dr. Syng Ill Lee for help and advice on carrying out membrane biotinylation studies.

REFERENCES

1. Payne, J. A., and Forbush, B., III (1995) *Curr. Opin. Cell Biol. 7*, 493−503.
2. Kaplan, M. R., Mount, D. B., and Delpire, E. (1996) *Annu. Rev. Physiol. 58*, 649−668.
3. Gillen, C. M., Brill, S., Payne, J. A., and Forbush, B., III (1996) *J. Biol. Chem. 271*, 16237−16244.
4. Evans, R. E., and Turner, R. J. (1998) *Biochem. Biophys. Res. Commun. 245*, 301−306.
5. Payne, J. A., Stevenson, T. J., and Donaldson, L. F. (1996) *J. Biol. Chem. 271*, 16245−16252.
6. Haas, M. (1994) *Am. J. Physiol. 267*, C869−C885.
7. Moore-Hoon, M. L., and Turner, R. J. (1998) *Eur. J. Morphol. 36*, 137−141.
8. Harling, H., Czaja, I., Schell, J., and Walden, R. (1997) *EMBO J. 16*, 5855−5866.
9. Gillen, C. M., Stirewalt, V. L., Bryant, D. A., and Forbush, B., III (1996) *Biophys. J. 70*, 204, abstract.
10. Moore-Hoon, M. L., and Turner, R. J. (1998) *Biochim. Biophys. Acta 1373*, 261−269.
11. Xu, J. C., Lytle, C., Zhu, T. T., Payne, J. A., Benz, E., and Forbush, B., III (1994) *Proc. Natl. Acad. Sci. U.S.A. 91*, 2201−2205.
12. Delpire, E., Rauchman, M. I., Beier, D. R., Hebert, S. C., and Gullans, S. R. (1994) *J. Biol. Chem. 269*, 25677−25683.
13. Payne, J. A., Xu, J. C., Haas, M., Lytle, C. Y., Ward, D., and Forbush, B., III (1995) *J. Biol. Chem. 270*, 17977−17985.
14. Lytle, C., and Forbush, B., III (1992) *J. Biol. Chem. 267*, 25438−25443.
15. Behnke, R. D., and Forbush, B., III (1998) *FASEB J. 12*, A1013, abstract.
16. Kurihara, K., Moore-Hoon, M. L., Saitoh, M., and Turner, R. J. (1999) *Am. J. Physiol. 277*, C1184−C1193.
17. Forbush, B., III, Payne, J. A., Xu, J. C., Biemesderfer, D., and Isenring, P. in *Abstracts of the International Society of Nephrology*, American Physiological Society, Bethesda, MD.
18. Isenring, P., Jacoby, S. C., Chang, J., Forbush, B., III (1998) *J. Gen. Physiol. 112*, 549−558.
19. Isenring, P., Jacoby, S. C., and Forbush, B., III (1998) *Proc. Natl. Acad. Sci. U.S.A. 95*, 7179−7184.
20. Isenring, P., and Forbush, B., III (1997) *J. Biol. Chem. 272*, 24556−24562.
21. Sachs, G., Shin, J. M., Briving, C., Wallmark, B., and Hersey, S. (1995) *Annu. Rev. Pharmacol. Toxicol. 35*, 277−305.
22. Fafournoux, P., Noel, J., and Pouyssegur, J. (1994) *J. Biol. Chem. 269*, 2589−2596.
23. Jennings, M. L. (1984) *J. Membr. Biol. 80*, 105−117.
24. Canessa, C. M., Schild, L., Buell, G., Thorens, B., Gautschi, I., Horisberger, J. D., and Rossier, B. C. (1994) *Nature 367*, 463−467.
25. Agre, R., Bonhivers, M., and Borgnia, M. J. (1998) *J. Biol. Chem. 273*, 14659−14662.
26. Manganel, M., and Turner, R. J. (1988) *J. Membr. Biol. 102*, 247−254.
27. O'Farrell, P. H. (1975) *J. Biol. Chem. 250*, 4007−4021.
28. Tanimura, A., Kurihara, K., Reshkin, S. J., and Turner, R. J. (1995) *J. Biol. Chem. 270*, 25252−25258.
29. Reshkin, S. J., Lee, S. L., George, J. N., and Turner, R. J. (1993) *J. Membr. Biol. 136*, 243−251.
30. Lytle, C., Xu, J.-C., Biemesderfer, D., Haas, M., and Forbush, B., III (1992) *J. Biol. Chem. 267*, 25428−25437.
31. Rothe, G. M., and Purkhanbaba, H. (1982) *Electrophoresis 3*, 33−42.
32. Lee, A. J., Bradford, J. M., Terris, J. M., Knepper, M. A., and Ecelbarger, C. A. (1997) *J. Am. Soc. Nephrol. 8*, 37, abstract.
33. Turner, R. J., George, J. N., and Baum, B. J. (1986) *J. Membr. Biol. 94*, 143−152.
34. Benjamin, B. A., and Johnson, E. A. (1997) *Am. J. Physiol. 273*, F473−F482.
35. Turner, R. J., and George, J. N. (1988) *J. Membr. Biol. 102*, 71−77.
36. Haas, M., and Forbus, B., III (1986) *J. Biol. Chem. 261*, 8434−8441.

BI992301V